77 (1948).
15. Method after H. Autrum [*Z. Vergl. Physiol.* **23**, 332 (1936)] and H. Markl and J. Tautz [*J. Comp. Physiol.* **99**, 79 (1975)]. These authors describe the acoustics of closed tubes like the one we used and illustrate how such tubes can be used in the analysis of insect hearing. Our tube had an inner diameter of 9.5 cm and was plugged on each end by a wooden piston, one of which contained an 8.5 cm dynamic loudspeaker. The bees gained access to the feeder inside the tube through a 3-cm hole that was plugged after the bee entered.
16. The tones were 3 s long, including gradual (1 s) onsets and offsets. The sound pressure and particle-movement amplitudes at the two sites were as follows: at the pressure maximum, 60-Pa (r.m.s.) sound pressure and 0.07-m/s peak particle velocity; and at the particle-movement maximum, 18-Pa (r.m.s.) pressure and 1.0-m/s peak particle velocity.
17. These were clearly not passive movements forced by the air oscillations. The antennae were moved over 2 mm upward and outward and the wings strongly retracted. The peak displacement of the air particles, for comparison, was 0.6 mm.
18. These response rates, each of which represents two responses out of 120 trials, probably reflect the "misfire" rate, the rate at which spontaneous movements of the bees happened to coincide in time with the sound and were therefore scored as positive responses.
19. The peak particle velocity within a few millimeters of a dancing bee is about 0.7 m/s (*2*).
20. We detected these currents with a small (3 mm) hair placed in the sound field and observed through microscope optics. The hair not only oscillated at the frequency of the sound but also was deflected by the currents.
21. H. Heran, *Z. Vergl. Physiol.* **42**, 103 (1959).
22. The bees that never reached the 50% response level are excluded (*13*) and did not undergo the discrimination procedure.
23. We thank D. R. Griffin for advice and technical help throughout, A. Michelsen and C. Sherrick for several useful suggestions and help in calibrating our transducers, M. Lindauer and J. L. Gould for encouragement and logistical support, F. C. Dyer for suggesting that we train bees with sounds and M. E. Bitterman that we try the Abramson technique, and C. Ristau and others for reviewing the manuscript. Supported by NSF grant BNS 85-09522 to J. L. Gould, and a grant from The Volkswagen Foundation to M. Lindauer.

29 November 1988; accepted 27 March 1989

Fibroblast Growth Factor in the Extracellular Matrix of Dystrophic (mdx) Mouse Muscle

J. DiMario, N. Buffinger, S. Yamada, R. C. Strohman*

Polyclonal antibody F547 reacts with a bovine basic fibroblast growth factor (bFGF) and a human recombinant bFGF, but not with bovine acidic fibroblast growth factor. This antibody localized bFGF in the extracellular matrix of mouse skeletal muscle, primarily in the fiber endomysium, which includes the heparin-containing basal lamina. In mdx mouse muscle, which displays persistent regeneration, FGF levels in the extracellular matrix are higher than those in controls. Overabundance of matrix FGF in mdx muscles may be related to an increase in both satellite cell and regenerative activity in the dystrophic muscle and may help explain the benign phenotype of mdx animals compared with the genetically identical human Duchenne muscular dystrophy.

Skeletal muscle regeneration depends on the presence of satellite cells embedded in the heparin-rich basal lamina of individual muscle fibers (*1*). During growth and maturation, and after injury in the adult, these stem cells are activated by unknown mechanisms, initiate cell division, and divide to generate a population of myoblasts that fuse to existing fibers to maintain constant ratios of nuclei to cytoplasm (during maturation) or fuse to form regenerated fibers (after adult injury) (*2*). Muscle myoblasts and satellite cells respond to FGF (*3*) and to other mitogens (*4*), and various muscles store an FGF-like activity (*5*). In addition, FGF and other growth factors bind strongly to heparin (*6*); FGF stimulation of myogenic cells is inhibited by heparin in cell cultures of both embryonic myoblasts and adult satellite cells (*7*). The negative regulation of satellite cell growth may therefore be related to heparin-FGF binding in the heparin-rich muscle basal lamina, and the positive response after injury may be related to a disruption of the heparin-FGF association (*8*).

However, to our knowledge, FGF has not been found in muscle basal lamina in vivo. Because of the persistent regeneration of mdx mouse muscle in comparison with its congenic normal strain, we looked for differences in FGF localization in muscle tissue. The mdx mouse (*9*) has the phenotype of a mild muscular dystrophy (*10*) but has the same X-chromosome gene mutation as the one responsible for Duchenne muscular dystrophy in humans and that is linked to an absence of the protein dystrophin within muscle fibers (*11*). Mdx fibers also lack dystrophin (*12*) but somehow escape the fatal phenotype characteristic of the human condition (*10, 13*). In normal mouse skeletal muscle, bFGF is localized around individual muscle fibers in areas identified as the fiber endomysium, the innermost component of which is the basal lamina. Moreover, in muscles from mdx animals the concentration of endomysial-bound FGF appeared amplified. The increase of FGF in the extracellular matrix of mdx muscles correlated with an increased regenerative activity in the muscles, which persists well into adult age (*10*).

We isolated and purified bovine bFGF by heparin-Sepharose chromatography (*6*). The purified protein was used as antigen to produce a polyclonal antibody to FGF (F547) in mice. It specifically stained bFGF but not bovine acidic FGF (aFGF) in an immunoblot (Fig. 1). This antibody also cross-reacted with human recombinant bFGF (Fig. 1) but not with other minor contaminants in our antigen preparation, and excess bFGF completely inhibited antibody reaction in frozen sections (Fig. 2). Thus, the antibody appears to be specific for bFGF.

Frozen sections of normal hind limb muscle that were stained with antibody F547 were examined microscopically (Fig. 2). All muscles were from 10-week-old animals. In the mdx mouse, the major burst of degeneration and regeneration takes place at 5 to 8 weeks (*10*), so that at 10 weeks the muscle has completed this initial regenerative re-

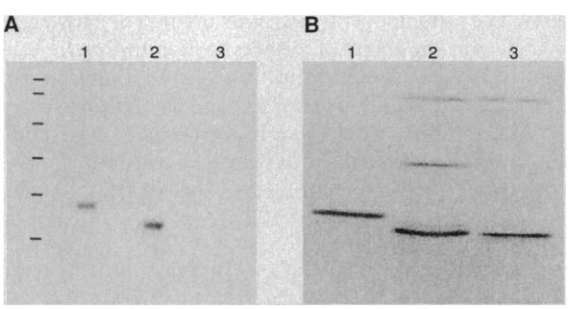

Fig. 1. (**A**) Immunoblot analysis of FGF preparations with antibody F547. The proteins were separated on a 12% SDS-polyacrylamide gel, transferred to nitrocellulose, and probed with F547 at a dilution of 1:200. Binding was visualized with a horseradish peroxidase staining kit (Vector Labs.). Protein molecular size markers (horizontal bars on the left) (Pharmacia LKB) are 94, 67, 43, 30, 20.1, and 14.4 kD. Lane 1, human recombinant bFGF, a full-length unmodified peptide; lane 2, bovine bFGF; lane 3, bovine aFGF. The bFGF and aFGF eluted at concentrations of 2*M* and 1*M* NaCl, respectively, from heparin-Sepharose affinity columns as described (*6*). Antibody F547 did not stain either laminin or fibronectin on similar protein immunoblots (*17*). (**B**) Stained gel of protein samples shown in (A). Stain was FAST-STAIN (Zoion Research, Allston, Massachusetts). Lane contents and electrophoresis conditions (*18*) were identical to those in (A).

Department of Zoology, University of California, Berkeley, CA 94720.

*To whom correspondence should be addressed.

sponse. In control muscles at 10 weeks, bFGF is localized to an area corresponding to the muscle endomysium (Fig. 2C). Fibers from mdx muscles at 10 weeks had an identical localization of bFGF, except that FGF levels in mdx muscle were greater than those in control muscle (Fig. 2D). The increase in the fluorescence signal from mdx sections, treated the same as control sections, is highly reproducible and was seen in all (four control and five mdx) animals examined. In addition, purified preparations of bovine bFGF completely extinguished reactivity of F547 with tissue sections (Fig. 2F). Finally, extraction of the tissue sections with 1*M* NaCl, which elutes aFGF but not bFGF from heparin-Sepharose (*6*), did not significantly alter antibody reactivity; extraction of sections with 2*M* NaCl, which does elute bFGF from heparin-Sepharose, abolished reactivity with F547 (Fig. 2, G and H).

Mdx muscles from 10-week-old mice also show increased numbers of small fibers and a high percentage (more than 85%) of fibers with central nuclei (Fig. 2B), features characteristic of muscle fiber regeneration (*10*). An increased presence of FGF in the fiber basal lamina area would thus be expected in a muscle in which continuous satellite cell activity is required. Even at 2 weeks of age, before the degeneration-regeneration cycle begins, more FGF was seen in fibers from mdx mice than in those of normal animals (Fig. 3). This finding suggests that increases in basal lamina–localized FGF result not from the degenerative-regenerative cycle but from some earlier event associated perhaps with the absence of dystrophin in the underlying muscle fiber membrane of mdx mice.

To date, bFGF has been localized to the basal lamina in muscle (Fig. 2) and in cornea (*14*), but the origin of this FGF is currently unknown. The synthesis and deposition of FGF in extracellular matrix by other cell types in vitro have been reported (*15*). Therefore, FGF could be deposited in the heparin-rich basal lamina by muscle cells early in fiber formation, or it could originate from the vascular endothelium or other cells (*15*). FGF bound into muscle extracellular matrix could be required for the continued low-level replication of satellite cells seen during early normal growth, when growing fibers maintain a constant ratio of nuclei to cytoplasm (*2*), and during regeneration, when new myonuclei must also be recruited from satellite cells located beneath the muscle basal lamina. The mechanisms that regulate FGF binding and release from heparin-rich basal lamina are not clear, but evidence exists for a heparin modulation of the FGF growth stimulus of myocytes in vitro (*7, 8*). FGF bound to basal lamina could easily be altered by the inflammatory response and by lymphocyte-related heparin-dissolving enzymes that are associated with muscle damage (*16*).

The increased levels of FGF in mdx muscle extracellular matrix may be related to the disease phenotype. In the mdx animal there is muscle degeneration at about 6 weeks of age, then persistent fiber regeneration for a year or more (*10*). Moreover, the regenerated muscle in the mdx animal exhibits lesions and central nuclei but remains fairly normal and without the massive necrosis seen in Duchenne muscular dystrophy. In Duchenne muscle there is a failure of regeneration and ultimate replacement of muscle by connective tissue and fat (*13*). The absence of dystrophin in mouse muscle sarcolemma (*12*) may lead to alterations in the juxtaposed basal lamina, resulting in enhanced FGF deposition and altered FGF-heparin

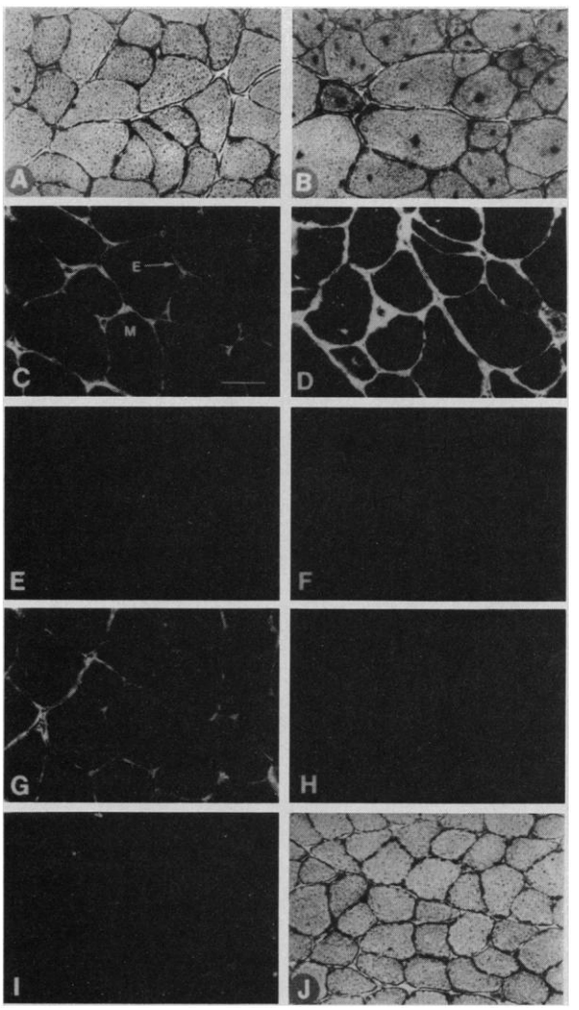

Fig. 2. FGF localization in frozen sections of mouse plantaris muscles at 10 weeks. Muscle tissue was immersed in Tissue-Tek (Miles) and frozen in liquid nitrogen. Tissues were sectioned at −20°C in a cryostat (Damon/International Equipment Company, Needham Heights, Massachusetts) at a thickness of 4 μm and collected on clean glass slides. Sections were incubated in 20 μl of F547 antiserum diluted to 1:100 in phosphate-buffered saline (PBS) (10 m*M* sodium phosphate and 150 m*M* NaCl, *p*H 7.2) for 2 hours at room temperature in a moist chamber, washed twice in PBS, incubated in fluorescein-conjugated goat antibody to mouse immunoglobulin G (Sigma) diluted to 1:20 in PBS, and washed again. *p*-Phenylenediamine in a mixture of PBS and glycerol (1:9) was added, and cover slips were applied. (**A**) Normal and (**B**) mdx muscle stained with Harris' hematoxylin. (**C**) Normal and (**D**) mdx muscle stained with antibody to FGF. (**E**) Normal muscle incubated in preimmune serum for 2 hours at room temperature. (**F**) Normal muscle stained with F547 that had previously been incubated with bFGF (20 μg) for 1 hour at 37°C. As an additional control, normal muscle was stained with F547 that had been incubated alone for 1 hour at 37°C, and normal fluorescence was observed. (**G**) Normal muscle incubated in 1*M* NaCl and 10 m*M* tris, *p*H 7.0, for 1 hour at 37°C before incubation with F547. (**H**) Normal muscle incubated with 2*M* NaCl and 10 m*M* tris for 1 hour at 37°C before incubation with the antibody. (**I**) Treatment of normal muscle section with heparinase (Sigma) followed by incubation with antibody. (**J**) Same as (H), but stained only with Harris' hematoxylin. In (C), M indicates muscle fiber and E arrow points to endomysium. Original magnification, ×500. Bar, 50 μm.

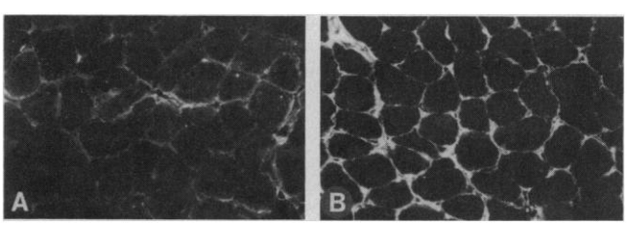

Fig. 3. FGF localization in mouse soleus muscle at 2 weeks. (**A**) Normal and (**B**) mdx muscle treated and stained with F547, as described in Fig. 2. FGF localization in control muscle at this age appears to be scanty and irregular, whereas in mdx muscle there is consistent staining around every fiber. Original magnification was the same as in Fig. 2, but fibers at age 2 weeks are smaller.

affinity. These changes in FGF might easily activate nearby satellite cells to divide and form new muscle fibers and could explain persistent regeneration observed in the dystrophic mouse. The mechanisms by which mdx mouse skeletal muscle escapes lethal phenotypes seen in Duchenne patients who have the identical mutation should provide clues to understanding and treating the human disease.

REFERENCES AND NOTES

1. A. Mauro, *J. Biophys. Biochem. Cytol.* **9**, 493 (1961); R. E. Allen, P. K. McAllister, K. C. Masak, *Mech. Ageing Dev.* **13**, 105 (1980); B. H. Lipton and E. Schultz, *Science* **205**, 1292 (1981).
2. F. P. Moss and C. P. LeBlond, *Anat. Rec.* **170**, 421 (1970); R. Bischoff, *Dev. Biol.* **115**, 129 (1986); U. Konigsberg, B. Lipton, I. R. Konigsberg, *ibid.* **45**, 260 (1975).
3. B. Olwin and S. Haushka, *Biochemistry* **25**, 3487 (1986); R. E. Allen, M. V. Dodson, L. S. Luiten, *Exp. Cell Res.* **152**, 154 (1984); D. Gospodarowicz, J. Weseman, J. S. Moran, J. Lindstrom, *J. Cell Biol.* **70**, 395 (1976); B. K. Lathrop, E. N. Olson, L. Glaser, *ibid.* **100**, 1540 (1985).
4. D. Z. Ewton and J. R. Florini, *Endocrinology* **106**, 577 (1980); J. R. Florini, *Muscle & Nerve* **10**, 577 (1987); E. Jennische, A. Skottner, A. Hannson, *Acta Physiol. Scand.* **129**, 9 (1987); T. A. Linkhardt, C. H. Clegg, S. Hauschka, *Dev. Biol.* **86**, 19 (1981).
5. E. Kardami, D. Spector, R. C. Strohman, *Dev. Biol.* **112**, 353 (1985); *Proc. Natl. Acad. Sci. U.S.A.* **82**, 8044 (1985); R. Bischoff, *Dev. Biol.* **115**, 140 (1986).
6. D. Gospodarowicz, J. Cheng, G. Lui, A. Baird, P. Bohlent, *Proc. Natl. Acad. Sci. U.S.A.* **81**, 6963 (1984); Y. Shing *et al.*, *Science* **223**, 1296 (1984); T. Maciag, T. Mehlman, R. Friesel, A. B. Schreiber, *ibid.* **225**, 932 (1984).
7. E. Kardami, D. Spector, R. C. Strohman, *Dev. Biol.* **126**, 19 (1988).
8. R. C. Strohman and E. Kardami, in *Cellular Endocrinology: Hormonal Control of Embryonic and Cellular Differentiation*, G. Serrero and J. Hayashi, Eds. (Liss, New York, 1986), pp. 287–296.
9. G. Bulfield, W. G. Siller, P. A. L. Wright, K. J. Moore, *Proc. Natl. Acad. Sci. U.S.A.* **81**, 1189 (1984).
10. J. Dangain and G. Vrbova, *Muscle & Nerve* **7**, 700 (1984); Y. Tanabe, K. Esaki, T. Nomura, *Acta Neuropathol.* **69**, 91 (1986); L. F. B. Torres and L. W. Duchen, *Brain* **110**, 269 (1987).
11. M. Koenig, E. P. Hoffman, A. P. Monaco, C. Feener, L. M. Kunkel, *Cell* **50**, 509 (1987); E. P. Hoffman, A. P. Monaco, C. C. Feener, L. M. Kunkel, *Science* **238**, 347 (1987).
12. E. P. Hoffman, R. H. Brown, L. M. Kunkle, *Cell* **51**, 919 (1987).
13. A. G. Engel, in *Myology*, A. G. Engel and B. Q. Banker, Eds. (McGraw-Hill, New York, 1986), pp. 1185–1202.
14. J. Folkman *et al.*, *Am. J. Pathol.* **130**, 393 (1988).
15. A. Baird and N. Ling, *Biochem. Biophys. Res. Commun.* **142**, 428 (1987); I. Vlodavsky *et al.*, *Proc. Natl. Acad. Sci. U.S.A.* **84**, 2292 (1987).
16. Y. Naparstek, I. R. Cohen, Z. Fuks, I. Vlodasky, *Nature* **310**, 241 (1984).
17. N. Buffinger and R. C. Strohman, unpublished results.
18. Width differences between lanes of Fig. 1A and Fig. 1B are due to use of a Miniblotter 16 (Immunetics, Cambridge, MA) in the immunoblot, which restricts antibody solutions to narrow strips along the length of the nitrocellulose membrane.

19. Human recombinant bFGF was provided by S. Hauschka and G. McKnight. Supported by NIH grant R01 AG02832 and a grant from the Muscular Dystrophy Association.

14 September 1988; accepted 3 March 1989

Corn and Culture in Central Andean Prehistory

SISSEL JOHANNESSEN AND CHRISTINE A. HASTORF

The prehistoric development and spread of domesticated maize varieties in the highlands of Peru, unlike the drier coastal deserts, is little known because ancient maize remains in this area survive mainly as fragments, kernels, and cob parts. An analysis of fragmented charred maize from prehistoric households (A.D. 450 to 1500) in the Mantaro Valley reveals a developmental sequence of maize varieties for Highland Peru. The evidence indicates an adoption of large-kernelled maize varieties beginning in the Late Intermediate (A.D. 1000). This is centuries later than a similar change in maize, associated with the Wari expansion, that occurred in coastal areas, and indicates minimal Wari impact in the Mantaro Valley.

DOMESTICATED MAIZE AND THE human groups that use it are interdependent. The hundreds of existing maize varieties are cultural artifacts created, maintained, used, changed, and moved by human groups (*1*, *2*). The study of prehistoric maize varieties is valuable to understanding the evolution of both maize itself and of the associated cultures.

Department of Anthropology, University of Minnesota, Minneapolis, MN 55455.

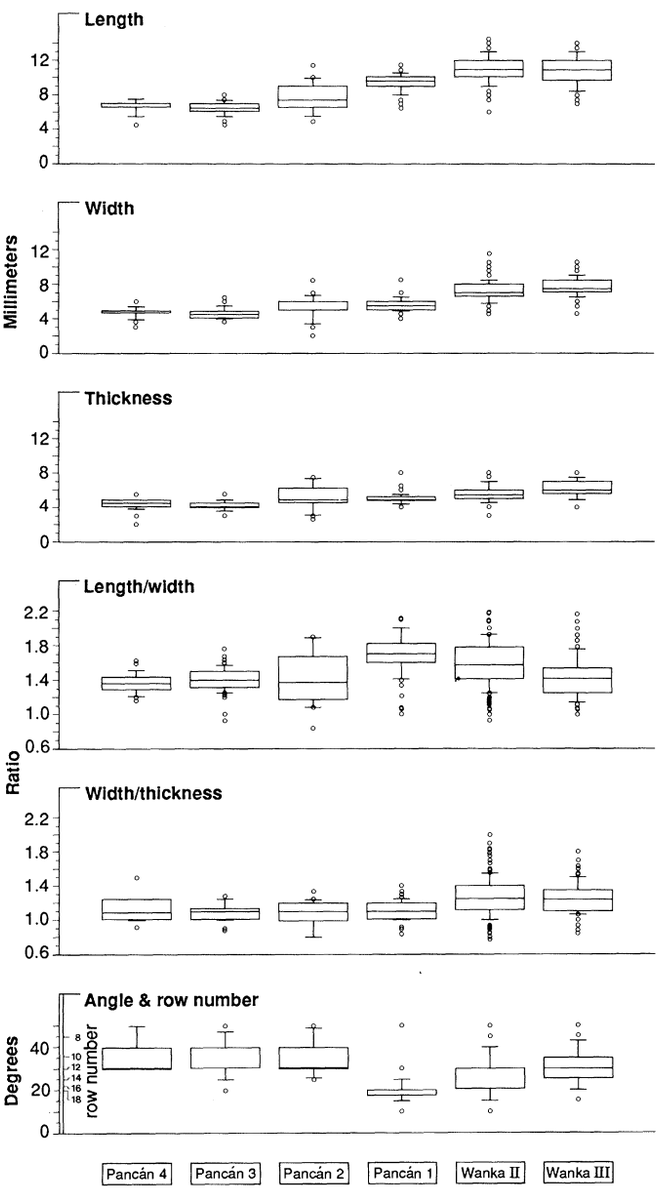

Fig. 1. Trends in kernel size, shape, and row number, showing distributions of kernel measurement values for six variables through time. The five lines in the percentile box plots mark the 10th, 25th, and 50th (median), 75th, and 90th percentiles. The small circles mark the <10th and >90th percentiles.